

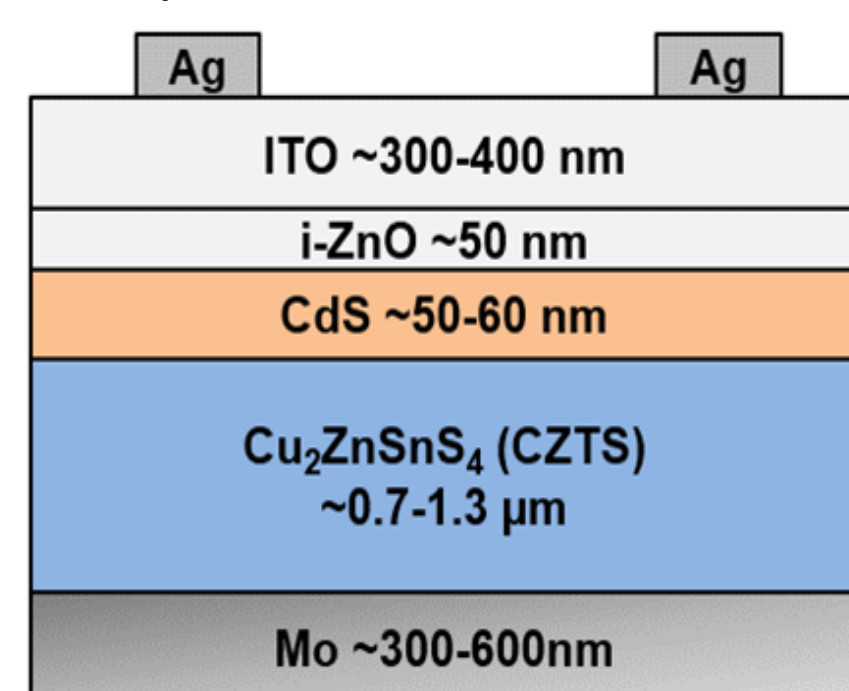
Development and Characterization of Copper Zinc Tin Sulfide (CZTS) Thin Films for Solar Cells Applications



Introduction

Current large-scale thin film solar cells require high production costs due to the limited and hard to supply materials like indium, gallium and tellurium [1]. In addition the extensive use of the toxic metal cadmium used in CdTe technologies has a negative environmental impact. In recent years, there has been extensive research focused on finding alternatives for thin film solar cells based on CIGS and CdTe technologies. The most promising result is the compound $\text{Cu}_2\text{ZnSnS}_4$ (CZTS), which is now a recognized potential material for the absorber layer in photovoltaic applications. The benefits of CZTS include the abundant and inexpensive supply of the materials directly reducing the cost of mass production, the nontoxic materials, and good photovoltaic properties with a band gap of 1.5 eV and an absorption coefficient greater than 10^4 cm^{-1} making CZTS an ideal candidate as an absorber layer in solar cells [2]. In past publications, Tauc plots based on absorption acquired from transmission measurements were used to estimate band gaps [1, 2, 3]. Since the absorber is typically prepared on a metal Mo film, using the transmission method might not be an effective method to determine optical band gap for these structure types. Spectroscopic ellipsometry is a non-contact technique, which has been used to determine the band gap for many films. Optical property of the bulk crystal CZTS, grown by the Bridgman method and studied with spectroscopic ellipsometry, has been reported by S. Levchenko [6]. However, in this study, spectroscopic ellipsometry will be used to measure CZTS's film thickness and their optical properties in CZTS/Mo/Glass stack with the Tauc-Lorentz model.

Four sample sets were investigated in this study: A, B, C, and D. Sample A and B were prepared first. Sample C and D were prepared at later stage. Each of sample set consist of at least two subsamples which originate from the same $1'' \times 3''$ CZTS precursor film and go through the annealing/sulfurization as a batch. One of the subsamples is then set aside for characterization of the CZTS film while the other(s) continue the process of becoming a cell, as shown below. Some characterization work, mainly with spectroscopic ellipsometry, will be reported here.

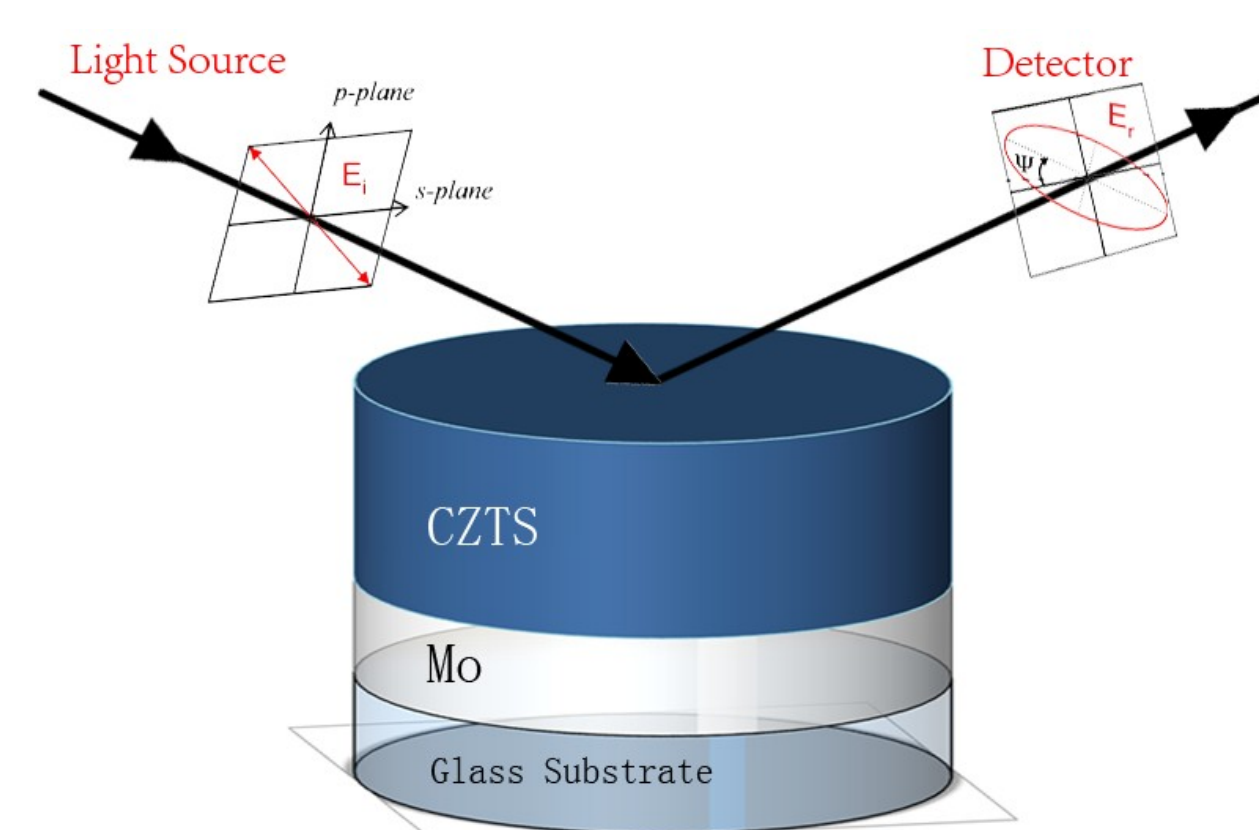


Experimental

Mo was sputtered via a bilayer method onto cleaned soda-lime glass substrates approximately $1'' \times 3''$ in size. Precursor layers for CZTS were then grown by magnetron co-sputtering via $2''$ diameter confocally positioned Cu, SnS, and ZnS targets at 3 mTorr chamber pressure, 13.5 cm target-to-substrate distance, and 100°C . The Cu, Sn, and Zn elemental concentrations in the films were controlled by varying the power supplied to the Cu, SnS, and ZnS targets. Samples were rotated throughout the deposition yielding CZTS precursor layers with good uniformity. Precursor layers were then annealed in a $\text{H}_2\text{S}/\text{N}_2$ (5%/95%) environment at atmospheric pressure for 4 hrs at 500°C in a quartz tube furnace in order to recrystallize the precursor films into the kesterite CZTS phase. The surfaces of the resulting CZTS layers were etched for a short time in HCl followed by NaCN to help reduce the presence of secondary phases at the CZTS/CdS interface.

Film Characterization

CZTS film thickness and optical constants N&K were obtained by using a spectroscopic ellipsometer TFProbe SE500BA, developed by Angstrom Sun Technologies Inc. The spectroscopic ellipsometry technique measures physical and optical properties on any section of the film without direct physical contact with the film surface. The TFProbe SE500BA detector covers a wavelength range from 250nm to 1700nm and is equipped with an advanced automatic variable incident angle precision goniometer. The CZTS samples were measured at 67.5, 70, and 72.5° degree incident angles with 512 wavelength points.



A Tauc-Lorentz dispersion model, calculated by the TFProbe 3.3 software, was applied on the measured data sets to obtain the optical properties of the CZTS films. The imaginary part of the dielectric function ϵ_i was developed by Jessison and Modine in 1996, by multiplying the Tauc joint density of states with the Lorentz oscillator:

$$\epsilon_i(E) = \frac{AE_0C(E-E_G)^2}{E((E^2-E_0^2)^2 + C^2E^2)}, \quad E > E_G$$

$$\epsilon_i(E) = 0, \quad E \leq E_G$$

where E_0 is the peak transition energy, C is the broadening term, E_G is the optical band gap, and A is proportional to the transition probability matrix element.

The real part of the dielectric function ϵ_r is calculated then by Kramers-Kronig integration:

$$\epsilon_r(E) = E_{\text{inf}} + \frac{2P}{\pi} \int_{E_G}^{\infty} \frac{\xi \epsilon_i(\xi)}{\xi^2 - E^2} d\xi$$

The fitting parameters in the software utilizes the variables A, C, E_0 , E_G and E_{inf} from the Tauc-Lorentz model.

When studying optical property over a very wide wavelength range, especially for photovoltaic films, the Tauc-Lorentz dispersion is inadequate to describe the dielectric response completely. Therefore, one or more Lorentz type oscillators were added into the total dielectric function in the analysis

$$\epsilon_r = \frac{A_1 \lambda^2 (\lambda^2 - L_0^2)}{(\lambda^2 - L_0^2)^2 + \gamma^2 \lambda^2}$$

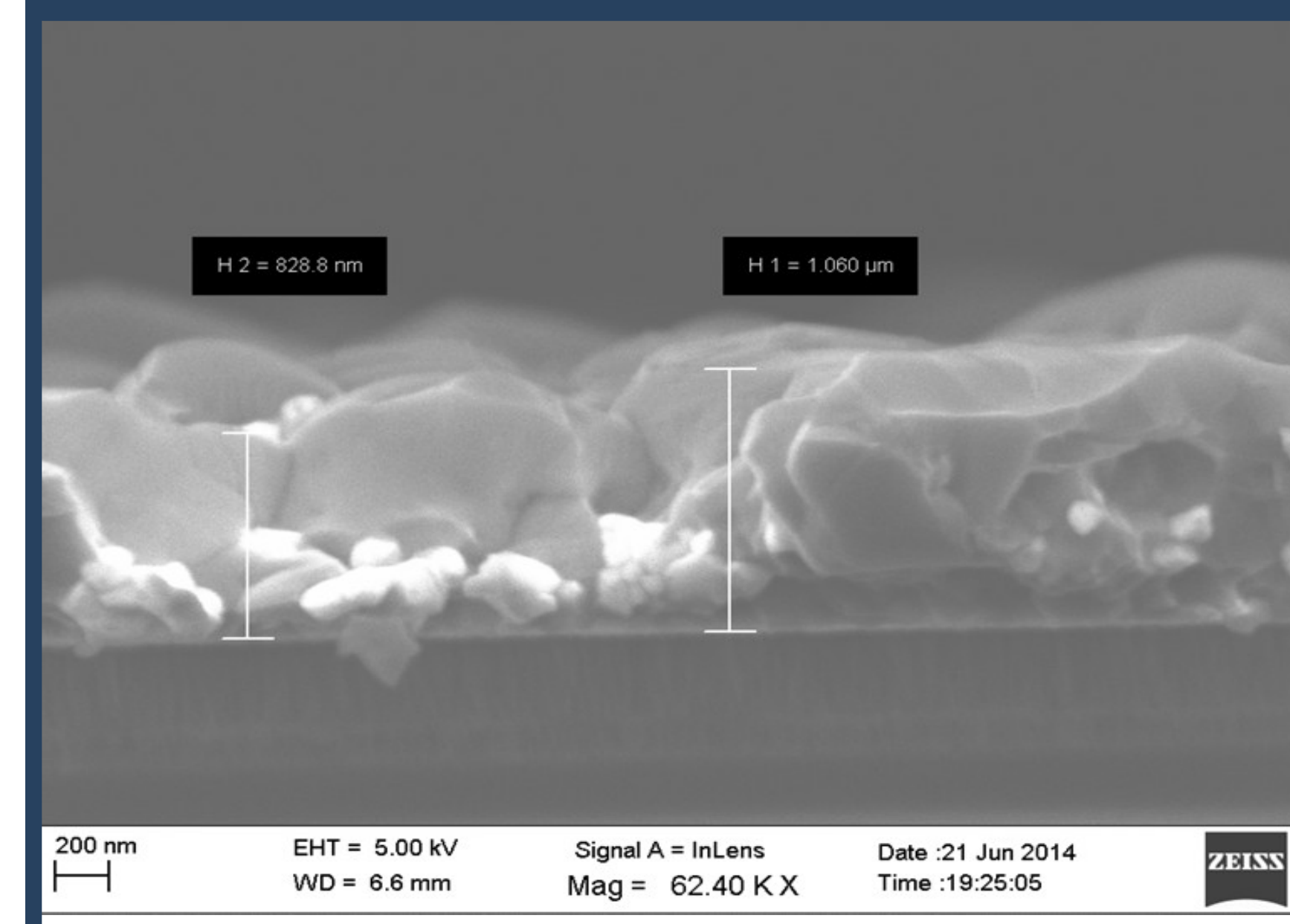
$$\epsilon_i = \frac{A_1 \lambda^3 \gamma}{(\lambda^2 - L_0^2)^2 + \gamma^2 \lambda^2}$$

where A_1 is the amplitude, L_0 is the central wavelength and γ is the width of the oscillators.

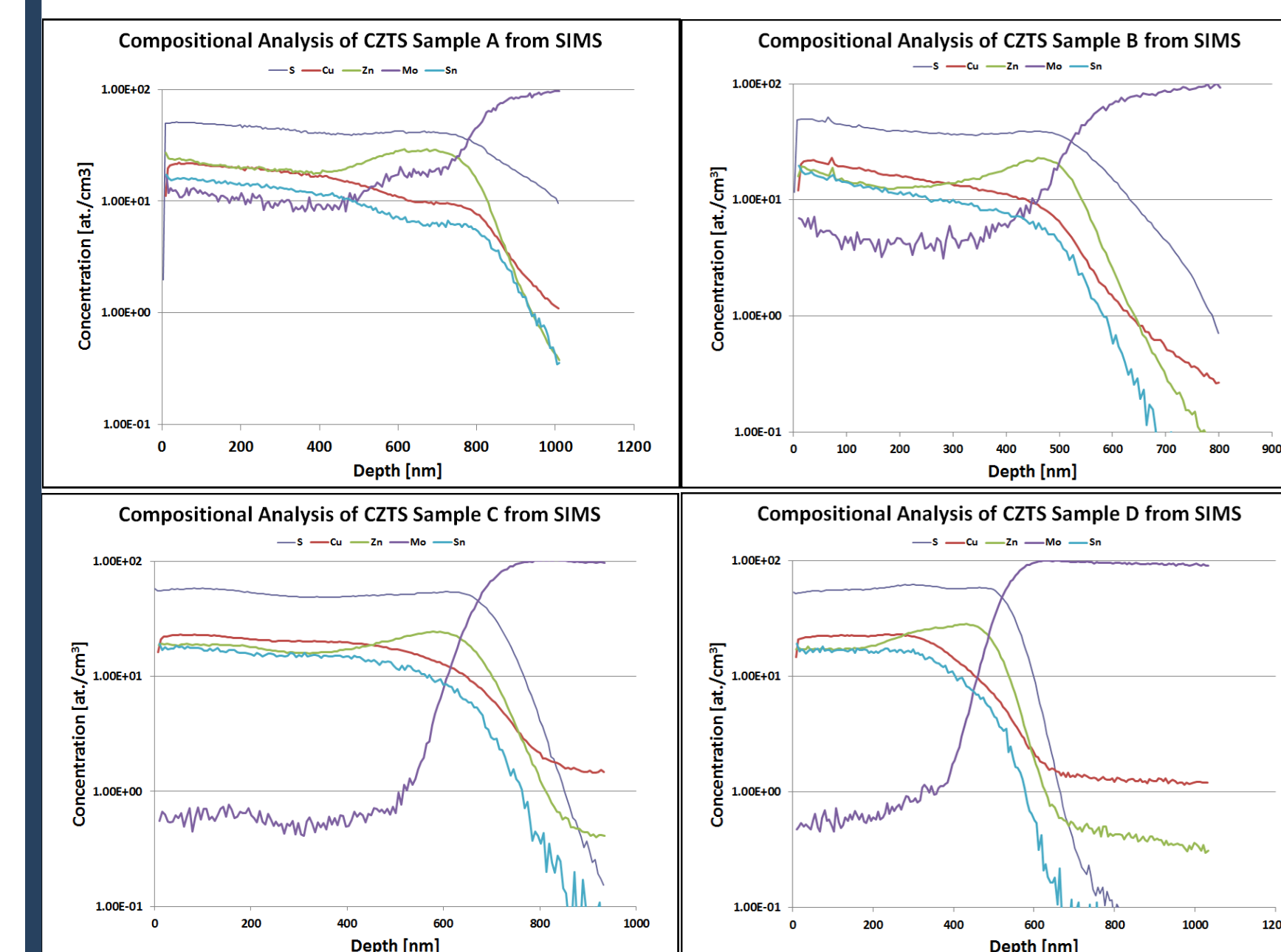
The Levenberg-Marquardt algorithm (LMA), a non-linear least-squares method, is used for modeling. The best fitted variables are found by minimizing the difference between the measured and model data.

TFProbe SR500 spectroscopic reflectometer was used for measuring each sample's reflection spectra. Scanning electron microscope (SEM) is utilized to examine the cross section of samples and also top surface to learn its structure. The secondary Ion Mass Spectrometry (SIMS) is applied to determine relative element compositions.

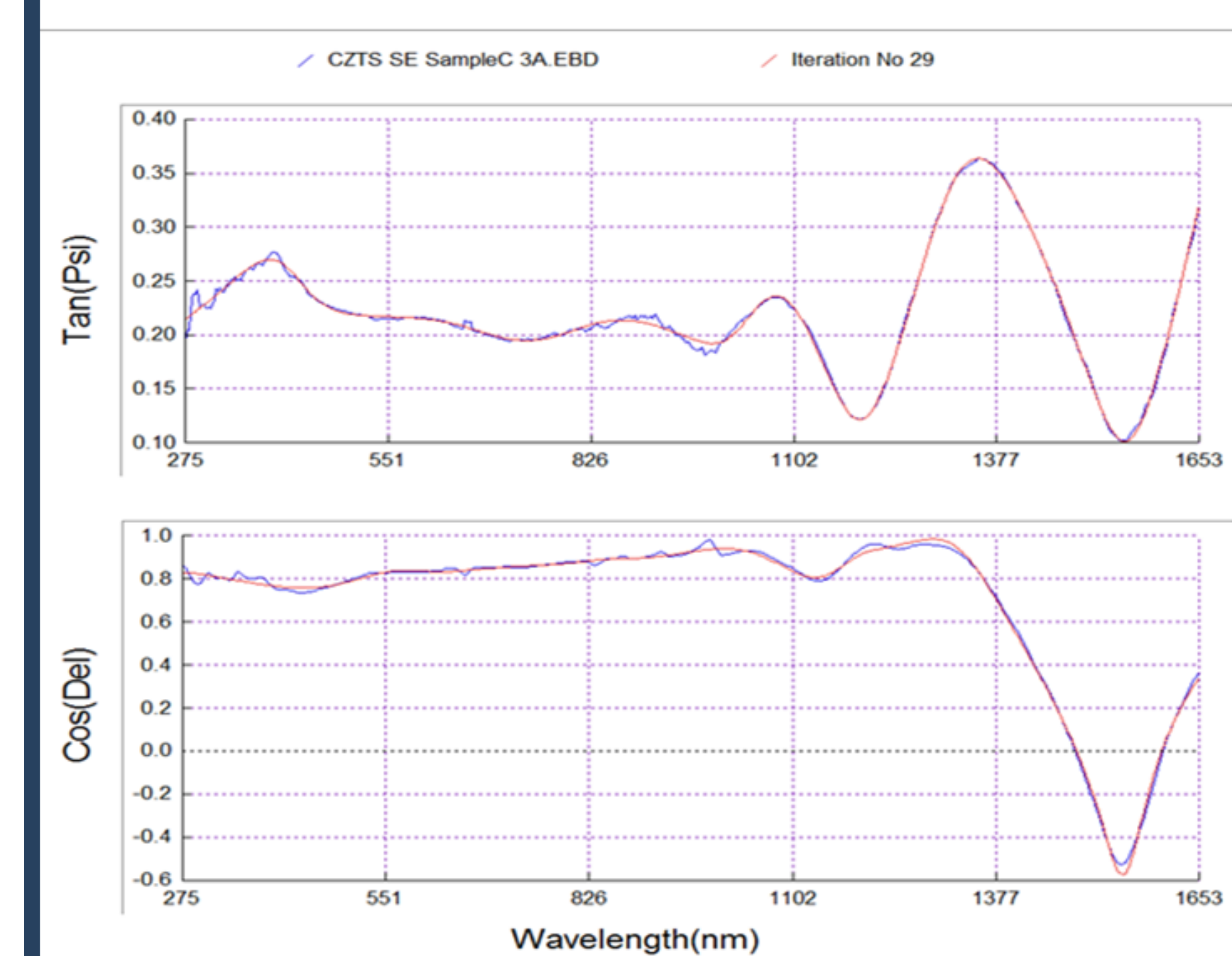
Results



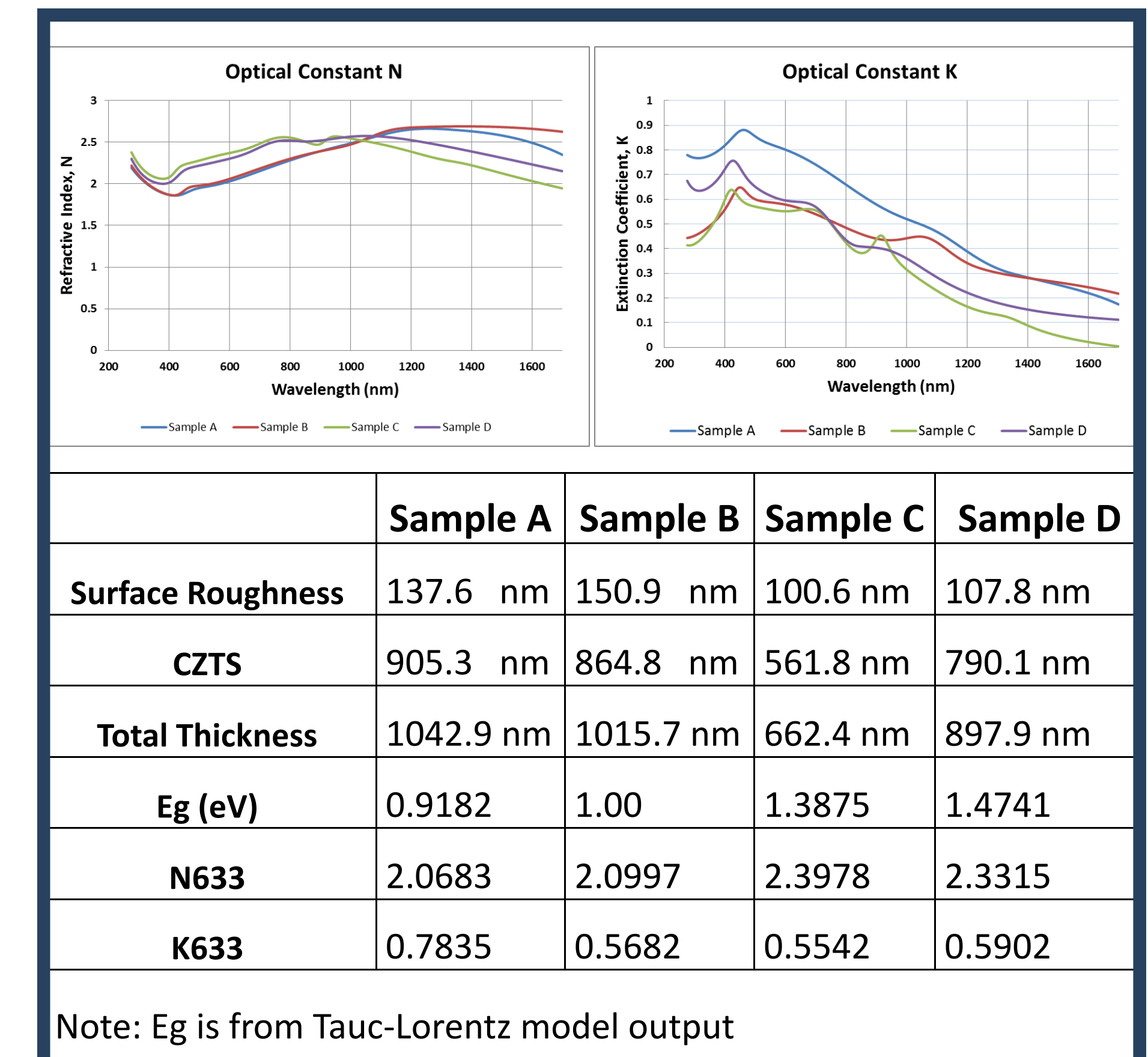
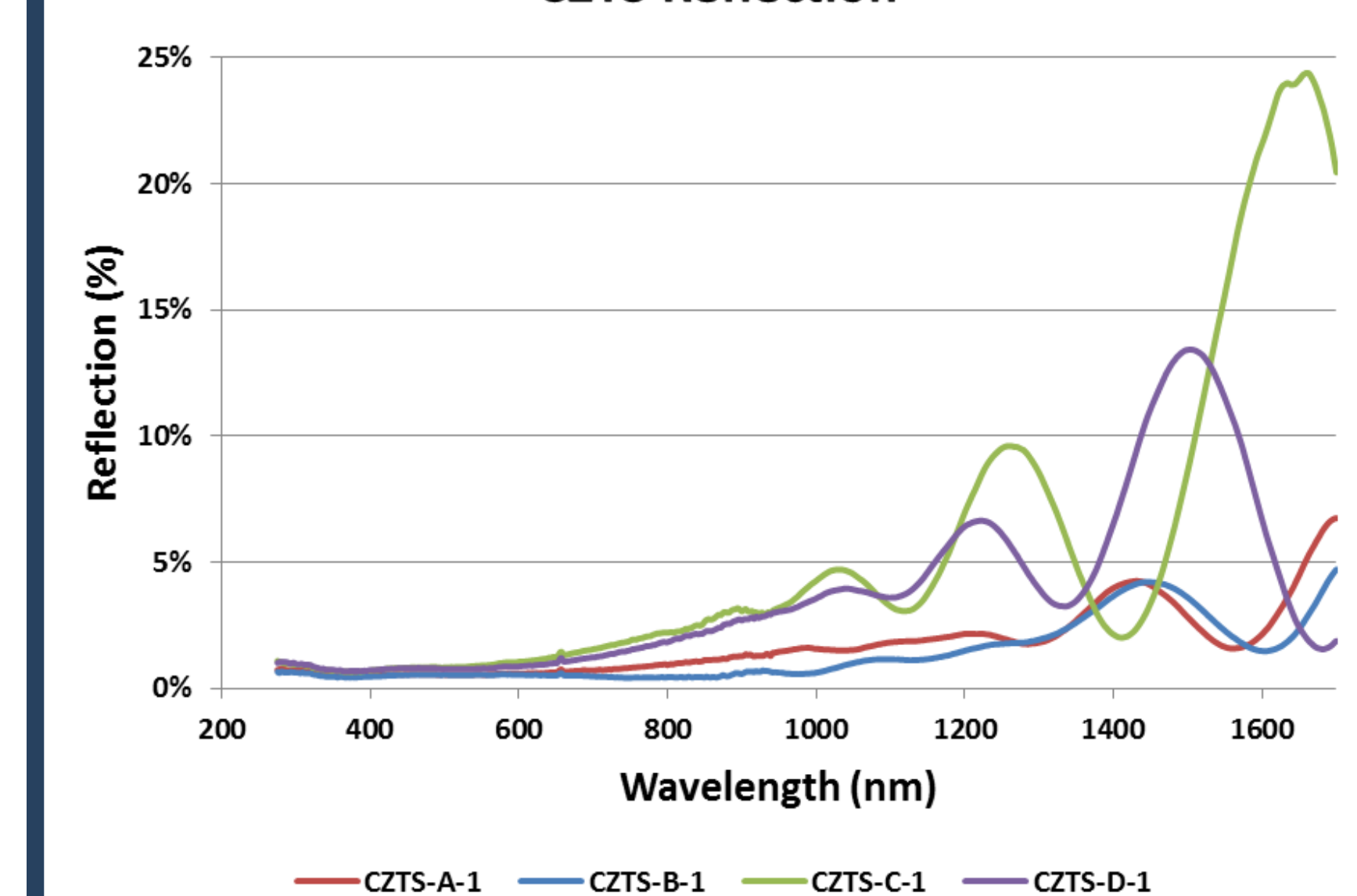
A typical Cross sectional SEM image shows CZTS layer of samples A. Large CZTS grains of 500+ nm and rough top surface are observed. The lighter regions near the CZTS/Mo interface are believed to be the ZnS phase.



A fitted graph for sample C at a 70° degree angle is plotted as shown below:



CZTS Reflection



Note: Eg is from Tauc-Lorentz model output

Discussion and Summary

- Total thickness measured with spectroscopic ellipsometry is consistent with cross sectional estimates from SEM. Spectroscopic ellipsometry model also revealed the same scale top surface roughness as shown from SEM examination.
- All profiles show similar compositions, with a Zn-rich layer at the base of the film.
- Older samples A and B have lower band gap values than expected. While Sample C and D have E_g values at 1.3875eV and 1.4741eV, respectively, which are close to reported 1.5eV for bulk CZTS
- The older samples A and B show more diffusion of Mo into the CZTS film than the newer samples (C & D). In Sample A, CZTS layer has about 25 at. % Mo in the region close to the Mo interface and about 10% Mo inside its top area. Sample B contains about 10% Mo in the CZTS layer. For newly prepared samples C and D, only about 1% Mo in the CZTS layer was found.
- Lower than expected band gap data by spectroscopic ellipsometry for sample A and B might be related to high content of Mo in the CZTS layer.
- The refractive indices (N) for both sample A and B are also lower than group Sample C and D. This could be caused by relatively lower packing density, higher surface roughness and excess Mo contents in CZTS layer.
- Reflection by Samples A and B is lower than samples C and D which could be related to surface roughness scale at their top surfaces of each sample.
- Present results shows spectroscopic ellipsometry is promising technique for directly determining CZTS's optical properties including its band gap in CZTS/Mo/Glass stack.

References

- Andersson, B.A., Materials availability for large-scale thin-film photovoltaics. K. Ito, T. Nakazawa, Jpn. J. Appl. Phys. 27 (1988) 2094.
Progress in Photovoltaics: Research and Applications, 2000. 8(1): p. 61-76.
Scofield, J., Duda, A., & Albin, D. (1995). Sputtered Molybdenum Bilayer Back Contact for Copper Indium Diselenide-Based Polycrystalline Thin-Film Solar Cells. Thin Solid Films, 260(1), 26-31.
Shin, B., Gunawan, O., & Zhu, Y. (2013). Thin film solar cell with 8.4% power conversion efficiency using an earth-abundant $\text{Cu}_2\text{ZnSnS}_4$. Progress in Photovoltaics: Research and Applications, 21(1), 72-76.
Wang, W., Winkler, M., Gunawan, O., Gokmen, T., Todorov, T., Zhu, Y., & Mitzi, D. (2014). Device Characteristics of CZTSSe Thin-Film Solar Cells with 12.6% Efficiency. Advanced Energy Materials, 4(7), 1301465.
X. Lin, et al., Thin Solid films (2012)